

radical(s). Second, the 6-yl radical (radical 4) decayed at about 300 K, probably into the 5-yl radical, as reported previously.¹² Specifically, no evidence was obtained that the (protonated) anion radical transformed into the 5-yl hydrogen addition radical.

Figure 5a shows the same EPR spectrum as that in Figure 1a. In Figure 5b is shown the spectrum obtained by simulation, including each of the resonances discussed above using the EN-DOR-determined hyperfine coupling tensors for the proton interactions obtained in the present work and the tensor for the nitrogen coupling of radical 6,¹² the 1-yl radical. The relative amount and the line width of each of the contributing radicals were adjusted to fit the experimental spectrum. However, the uncertainties using this procedure are considerable, as several of the resonances are partly or completely hidden under the far more intense EPR resonance of radical 3. Since g tensors were not measured, all resonances contributing to Figure 5b were given a common g value of 2.0023. This is the main reason for minor asymmetries in the experimental spectrum which are not reproduced in the calculated one. In spite of the approximations, the reconstructed spectrum nicely accounts for the main features of the experimental spectrum.

Clearly, radical 2 is the charge-neutralized reduction product of thymine. The presence of radical 6, the 1-yl radical, strongly suggests that this species is the oxidation product of the thymine base, deprotonated at N1. Anhydrous thymine crystals are largely nonpolar, particularly in the regions around the methyl group. Electron-hole geminate recombination is likely to be an important event in such matrices, an event that results in (super)excited molecules. Homolytic scission of nonpolar C-H bonds is a most probable result of such an event, and the hydrogen dissociated is expected to be from the methyl group. The hydrogen atoms thus formed may either (a) abstract a hydrogen from a neighboring methyl group, thus forming the radical pairs together with molecular hydrogen, or (b) add to a neighboring molecule. Hydrogen atoms preferentially add to the C6 position of the thymine base, forming 5-yl radicals¹ (radical 5), but possibly also some of the 6-yl radicals (radical 4) may be formed this way. Our results show that O4 is a more probable site for protonation of the anion (in solids) than C6.^{1,5,22} However, C5 is the preferred

position for proton addition to the parent thymine base.⁷ Consequently, the 6-yl radicals formed at low temperatures are probably not due to direct H addition but rather to protonation of the parent molecule at C5 from protons released to the lattice during radiation, followed by electron capture. Due to the large population of radical pairs in this crystal, (a) seems to be the predominant reaction.

The mechanisms above are like those proposed for thymidine and 1-methylthymine.⁷ In all cases, the protonated anion was formed at low temperature and decayed at about 40 K. It appears from the study of Ta that the tendency for protonation at O4 even at very low temperatures is so strong that it occurs whether O4 is hydrogen bonded or not. In both thymidine and 1-methylthymine, N1 is bonded to a non-hydrogen atom. The primary cation must deprotonate either at the C1 position (in thymidine) or at the C5 methyl group. From studies of frozen thymine solutions it has been shown that the 7-yl radical may act as the successor for initially formed cations.²³ Consequently, in thymidine and in 1-methylthymine, radical 3 may be formed both by deprotonation of the cation and by direct hydrogen abstraction. In the case of deprotonation, the ejected proton is a nonexchangeable one. In studies using partially deuterated crystals the products subsequent to the addition of this nonexchangeable proton, and those following direct hydrogen addition, are indistinguishable.⁷ In anhydrous crystals of thymine, this ambiguity could possibly have been solved since radical 6, the 1-yl radical, presumably is the deprotonated cation and the HN1 proton is an exchangeable one. However, in the present work, partially deuterated crystals were not investigated.

Acknowledgment. This work was supported by NIH Grant CA 36810 and by NATO Travel Grant RG 0426/88. Additional support (to E.S. and E.O.H.) was obtained from Department of Physics and Astronomy, Georgia State University, and from Norges Allmennvitenskapelige Forskningsråd (NAVF).

(22) Deeble, D. J.; Das, S.; von Sonntag, C. *J. Phys. Chem.* 1985, 89, 5784.
(23) Sevilla, M. D.; Van Paemel, C.; Zorman, G. *J. Phys. Chem.* 1972, 76, 3577.

Sonochemistry: Some Factors That Determine the Ability of a Liquid To Cavitate in an Ultrasonic Field

Arnim Henglein,* Daniel Herburger, and Maritza Gutiérrez

Hahn-Meitner-Institut Berlin GmbH, Bereich S, Postfach 390128, Glienicke Strasse 100, D-1000 Berlin 39, Germany (Received: July 30, 1991)

Aqueous luminol solutions are irradiated with a 5-ms pulse train of 1-MHz ultrasound (on:off ratio 1:10), and the luminescence pulse train generated is recorded. The first pulses of the train produce chemiluminescence less efficiently than the later ones. The critical number of pulses, N_{crit} , which has to be applied until the full luminescence signal is developed increases moderately with increasing preirradiation by continuous ultrasound until a very steep increase occurs at a critical time, t_{crit} . At this point, the solution is practically devoid of nuclei capable of inducing cavitation. Similarly, N_{crit} increases moderately with decreasing gas content of the solution (produced by evacuation, but irradiation under full atmospheric pressure) until at about 80% gas concentration a steep increase in N_{crit} occurs again. The results are explained in terms of nuclei $X_n(g)$ (gas pockets stabilized in crevices of microscopic solid dust particles) which are needed for the initiation of chemically effective cavitation. These nuclei are very efficiently destroyed by ultrasound. They are also removed by decreasing the concentration of molecularly dissolved gas in the liquid. However, the ultrasound itself also produces short-lived nuclei X_u (free microbubbles) which can initiate cavitation.

Introduction

The chemical effects of ultrasound in liquids are brought about by cavitation, a prerequisite for the occurrence of cavitation being the presence of a dissolved gas. Monoatomic and diatomic gases are often most effective because the large specific heat ratios of

these gases are favorable for obtaining high temperatures in the oscillating or collapsing gas bubbles produced in an ultrasonic field.¹ It has recently been shown by using ultrasonic pulse trains

(1) Neppiras, E. A. *Phys. Rep.* 1980, 61, 159.

that the chemical effects are not immediately initiated, since a certain induction time is required for the tiny bubbles produced to reach the resonance size.² In these investigations, aqueous luminol solutions were irradiated with pulse trains, and the resulting luminescence trains recorded by appropriate electronic means. The analysis of the shape of the luminescence pulses showed that the first pulses of the train were quite different from the later ones. The early luminescence train pattern indicates how readily the liquid is able to develop chemically active cavities upon ultrasonic irradiation.

In the present paper, the ability of the solution to cavitate under various conditions is studied using the luminescence pulses as indicator. These various conditions include (1) aging of the solution, (2) preirradiation with ultrasound, (3) partial degassing by evacuation, and (4) the effects of regassing. An important experimental point should be emphasized: in some cases the measurement of the cavitation behavior of the solution was carried out at different gas concentrations but under the full atmospheric gas pressure during the irradiation. This measurement can only be carried out in a "short-irradiation" experiment, since longer irradiation leads to a change in gas concentration due to the uptake of gas from the atmosphere as a consequence of the agitation caused in the liquid.

The light emitted from irradiated luminol solutions is chemiluminescence, a consequence of the oxidation of luminol by OH radicals generated in the cavitation bubbles. This luminescence is stronger by almost 2 orders of magnitude than the sonoluminescence observed in water which is mainly caused by emission from excited radicals.^{3,4} We have also carried out experiments on the sonoluminescence of water; the same pulse patterns were found as in the luminol-containing solutions.

Experimental Section

The irradiation setup and data acquisition system have previously been described.² The 1-MHz ultrasound was emitted vertically from a quartz transducer into a glass vessel which contained 25 mL of solution. The vessel had a planar bottom with $\lambda/2$ thickness. The luminescence signals were recorded by a photomultiplier positioned near the vessel.

The luminol solution was sonicated under air. To follow the degassing by the ultrasonic treatment, a tiny oxygen-sensitive electrode was used to measure the O_2 concentration at various irradiation times. The electrode was mounted in such a way that it could be pulled out of the solution during irradiation (to prevent damage to the electrode) and pushed back into the solution immediately after irradiation. The equilibration time of the electrode was 2 min, i.e., much shorter than the time required for noticeable regassing by diffusion of air into the irradiated liquid. Making the plausible assumption that nitrogen is liberated from the air-containing solution at the same rate as oxygen, the measurement of the decrease in oxygen concentration can be regarded as a determination of the rate of air loss due to the degassing action of the ultrasound.

In most of the experiments, an ultrasonic train of 5-ms pulses was applied, the interval between the pulses being 10 times longer (on/off ratio: 1:10). Thus, $1/(5 \times 10^{-3} + 5 \times 10^{-2})$ or close to 18 pulses were applied per second. Each pulse consisted of 5000 oscillations of the 1-MHz ultrasound.

The various intensities used are characterized by the high-frequency (hf) power picked up by the transducer. At 60 W of hf power the intensity was about 1 W/cm^2 as determined by measuring the rate of the temperature increase of the liquid upon irradiation with continuous ultrasound.

Results

Aging Effects. We prepared 2 L of solution using water fresh from a millipore-ion-exchange column. Luminol (5-amino-1,2,3,4-tetrahydrophthalazin-1,4-dione, 800 mg) and NaOH (4.8

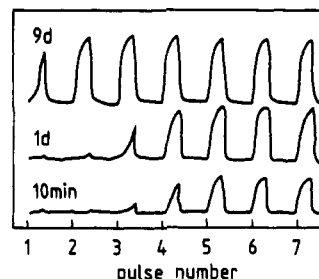


Figure 1. Shape of the first seven luminescence pulses upon the application of a 5-ms ultrasonic pulse train to a solution which was aged for various times.

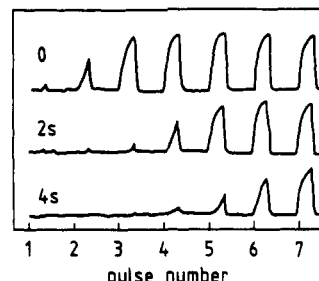


Figure 2. First seven luminescence pulses at various times of preirradiation. hf power: 40 W.

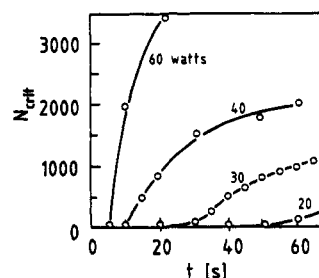


Figure 3. Critical number of pulses as a function of the time of preirradiation for various hf powers.

g) were dissolved and the solution kept in a glass bottle closed with a glass joint. Aliquots of 25 mL were transferred with a pipette into the irradiation vessel.

The luminescence pulses depended on the age of the solution as can be seen from Figure 1, where the first seven luminescence pulses are shown for different aging times after the preparation of the solution. Note that the interval time between the pulses is not correctly given. The first two pulses produced practically no chemical effect in the freshly prepared solution (10 min), the third pulse had a small effect, the fourth pulse was more efficient, and the later pulses reached the peak efficiency, i.e., a stationary state. The solution which was aged for one day showed slightly improved cavitation behavior, as the second pulse already produced a noticeable effect, and the third pulse was more efficient than in the freshly prepared solution. After 9 days of aging, the first pulse was already chemically active, although not as efficient as the later ones. Note also that the maximum luminescence reached in the later pulses became greater with increasing time of aging.

The following experiments were carried out with solutions that were aged for 2 days.

Effects of Preirradiation. In the experiments of Figure 2, the solution was preirradiated with continuous ultrasound for various times, and the 5-ms pulse train applied shortly after this treatment. It can be seen that a 2-s preirradiation affected the luminescence noticeably as the full activity was not reached before the fifth pulse. After a 4-s preirradiation the full luminescence signal was not developed until the seventh pulse. The critical number of pulses required to reach the full luminescence activity is designated by N_{crit} .

In Figure 3, N_{crit} was determined as a function of preirradiation time at various hf powers picked up by the transducer. Preirra-

(2) Henglein, A.; Ulrich, R.; Lilie, J. *J. Am. Chem. Soc.* **1989**, *111*, 1974.

(3) Sehgal, C.; Sutherland, R. G.; Verrall, R. E. *J. Phys. Chem.* **1980**, *84*, 388.

(4) Suslick, K. S.; Doktycz, S. J.; Flint, E. B. *Ultrasonics* **1990**, *28*, 280.

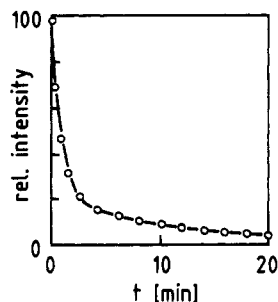


Figure 4. Luminescence intensity as a function of the time of continuous irradiation (60 W).

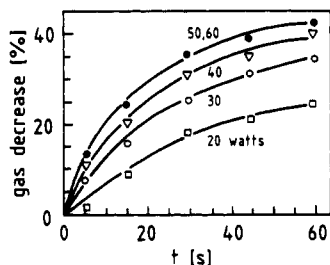


Figure 5. Decrease in air content by continuous irradiation at various hf powers.

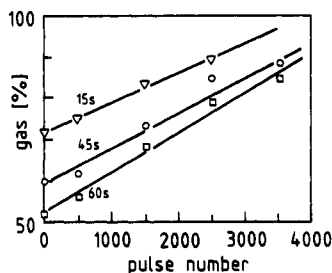


Figure 6. Preirradiation of a solution at 60 W for 15, 45, and 60 s; subsequent application of the pulse train: gas concentration as a function of the pulse number.

diation times much longer than those in Figure 2 were applied. It can be seen that N_{crit} increases very steeply at a critical time of preirradiation, which we call t_{crit} and which becomes shorter with increasing intensity of the ultrasound. For example, $t_{crit} = 5$ s at 60 W, 10 s at 40 W, and 30 s at 30 W. At shorter times, $t < t_{crit}$, the critical pulse number moderately increases as already shown in Figure 2 (this increase cannot be seen on the very compressed ordinate scale in Figure 3).

The full signal of the later pulses in Figure 2 is smaller for longer preirradiation times. This effect is probably not related to the loss of gas. It has already been found previously that the luminescence of luminol solutions decreases with increasing sonication time.² This can also be seen from Figure 4, where the temporal changes in luminescence intensity under continuous sonication are shown. The effect is attributed to the formation of a product from the oxidation of luminol in the early stages of irradiation which quenches the luminescence in the later stages.²

Degassing and Regassing. It is important for the interpretation of the phenomena to know the rate of degassing of the solution. Figure 5 shows the decrease in air concentration (in percent of the saturated solution) as a function of time for the irradiation with continuous ultrasound. It can be seen that the liquid is degassed more rapidly with increasing intensity. However, as intensities above 50 W, there was no further increase in the rate. At these intensities a fountain forms in the solution, together with fog, which facilitates the uptake of gas from the atmosphere, the degassing action being counterbalanced to a certain degree.

When a solution which had been preirradiated continuously was then exposed to the 5-ms pulse train, partial regassing took place. This can be seen from Figure 6, where the gas concentration

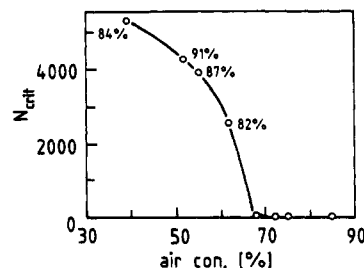


Figure 7. Critical number of pulses as a function of the air concentration (60 W). The air concentration given on the experimental points was determined when the full luminescence signal had been developed.

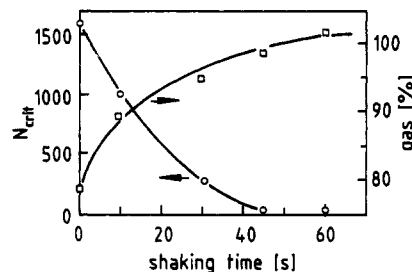


Figure 8. Cavitation recovery of a solution which had been sonicated for 30 s at 40 W. Critical pulse number and gas content as functions of shaking time.

(in percent of the saturated solution) is plotted as a function of the number of pulses applied. The solution was preirradiated for 15, 45, and 60 s at 60 W.

In the experiments of Figure 3, degassing occurred during the continuous preirradiation and regassing to a certain degree during the subsequent exposure to the pulse train. It is interesting to note the gas content of the solution at the critical times: at $t_{crit} = 5$ s (60 W) the gas content was 85%, at $t_{crit} = 10$ s (40 W) it was 84%, and at $t_{crit} = 30$ s (30 W) it was 75%. It can thus be said that N_{crit} starts to increase steeply when the gas concentration of the saturated solution has decreased by roughly 20% during the continuous preirradiation. The gas concentration was also measured immediately after the application of N_{crit} pulses for various preirradiation times $t > t_{crit}$, i.e., long enough that the loss of gas from the solution was much greater than 20%. It turned out that the application of N_{crit} pulses had led to a certain amount of regassing to produce gas concentrations between 84 and 90%. The 80% content thus appears as a significant limit for the efficient initiation of cavitation.

Effects of Gas Content. In the experiments of Figure 7, the luminescence was investigated for solutions containing different gas concentrations. A sample of the solution was degassed by evacuation with a water pump. Various mixtures from this degassed solution and the gas containing solution were prepared and irradiated with the 5-ms pulse train. The gas content of the mixtures was checked before irradiation by the oxygen-sensitive electrode. Figure 7 shows N_{crit} as a function of the percentage of air in the mixture. It can be seen that N_{crit} changes little when the concentration is decreased from 100 to about 70%. At smaller air concentrations, the critical number of pulses increased drastically. The air concentration in the liquid was also determined after the onset of the full luminescence signal. This concentration is noted next to the experimental points in Figure 7. It can be seen that the luminescence was fully developed after the air concentration reached about 80% during regassing by the pulse train.

In the experiments of Figure 8, the solution was continuously preirradiated for 30 s. After this time, the gas content had dropped to 80%. N_{crit} was as high as 1600. The irradiated solution was now treated in a shaking apparatus in order to regas it. Figure 8 shows how the gas content increased upon shaking. It also shows that N_{crit} decreased with increasing shaking time. After about 50 s, the gas content was fully restored and N_{crit} was as low as in the original solution.

Discussion

Stable and Unstable Nuclei. Cavitation in a liquid can be brought about only in the presence of inhomogeneities that serve as preferential sites for liquid rupture. Tiny gas bubbles of microscopic dimensions are generally regarded as the effective nuclei. However, such microbubbles are inherently unstable towards dissolution due to surface tension. Among the various models for the stabilization of such bubbles, the conical crevice model seems to be the most widely accepted one.⁵ The model postulates that a liquid contains solid particles of microscopic dimensions which have a rugged surface and are able to stabilize a tiny gas pocket in a crevice. Let us designate such nuclei as $X_n(g)$, the index n indicating that they occur naturally in a liquid, and the g in parentheses indicating that the nucleus carries a gas pocket. Some previous observations led us to postulate that ultrasound not only produces chemically active cavitation on these nuclei but at the same time destroys them:^{2,6} the microbubble is detached from the solid particle, grows by rectified diffusion^{7,8} in the ultrasonic field, undergoes violent oscillation, and finally collapses after having reached the resonance size. During these oscillations and the collapse the high temperatures are produced (in the adiabatic compression phase) that are responsible for the initiation of the chemical reactions. Two kinds of destruction of the $X_n(g)$ nuclei can be conceived: (1) after a nucleus is emptied of its gas pocket, it no longer acts as a nucleus for the inception of cavitation unless it is refilled by gas; (2) the solid particle may be fragmented mechanically under the influence of the hydrodynamic shear forces existing near oscillating bubbles, and the fragments may no longer be able to stabilize microbubbles.

A second type of nuclei which are produced by the ultrasound itself are the free microbubbles that are formed during the collapse of a resonating bubble. Let us designate these nuclei, which are unstable, by X_u , the index u indicating their formation by ultrasound. Once the ultrasound has initiated cavitation on $X_n(g)$ nuclei, cavitation still continues to occur at longer irradiation times despite the destruction of the $X_n(g)$'s, as the X_u 's are being produced continuously. When the ultrasound is applied as a train of pulses, the inception of cavitation can be hampered, if the interval time between the pulses is longer than the life time of the X_u nuclei.^{2,6} These bubbles can disappear via dissolution or—more probable at higher intensities, i.e., greater bubble concentrations—via coalescence to form larger bubbles which are no longer chemically active.

The 5-ms pulses are just long enough to build up maximum cavitation. This can be recognized from the shape of the later pulses in Figures 1 and 2. The ultrasonic pulses were rectangular. However, a luminescence pulse grew in more slowly. The 5-ms pulses are not long enough to allow much luminescence to build up in the first pulse or the first few pulses. More and more X_u nuclei accumulate during the first pulses until the concentration of these nuclei is large enough to ensure that the later pulses generate the full luminescence.

The preirradiation by continuous ultrasound (Figures 2 and 3) causes an increase in the critical number of pulses, N_{crit} , required to reach the final luminescence intensity. This is attributed to the destruction of $X_n(g)$ nuclei by the preirradiation. In the beginning, the effect is not dramatic: N_{crit} increases moderately with the preirradiation time. However, at times longer than the critical time, t_{crit} , the critical pulse number drastically becomes greater. The ability of the liquid to cavitate is rather suddenly decreased at $t = t_{crit}$. This is attributed to a total consumption of $X_n(g)$ nuclei.

Stable Nuclei and Total Gas Concentration. In the foregoing discussion, the destruction of nuclei $X_n(g)$ and the changes in the total gas concentration were regarded as two independent parameters that determine the ability of a liquid to cavitate.

However, the question has to be asked: does a change in gas concentration, for example by evacuation, also lead to a change in the concentration of active nuclei $X_n(g)$? It seems plausible to assume that the gas trapped in a crevice is in equilibrium with gas molecules truly dissolved in the liquid. This equilibrium may be written as



where $X_n(g)$ means an active nucleus carrying trapped gas, X_n is an inactive nucleus that has lost its gas microbubble, and g_m is molecularly dissolved gas. In a saturated solution, the $X_n(g)$ nuclei are most stable. As the concentration of gas g_m is decreased, the equilibrium of eq 1 is shifted to the right side, i.e., more and more nuclei lose their gas pocket. The concentration of $X_n(g)$ nuclei is already extremely small when about 30% of the gas in the liquid is removed, if we interpret the steep increase in N_{crit} in Figure 7 as the point where the solution is practically depleted of $X_n(g)$. The action of the pulse train would then primarily serve to increase the gas concentration by agitating the liquid, the corresponding left shift of the equilibrium of eq 1 leading to the reformation of $X_n(g)$ nuclei on which the pulses can then initiate chemically active cavitation.

The steep increase in N_{crit} occurred in the experiments of Figure 3 at a preirradiation time at which only about 20% of gas had been released from the liquid. This means that removal of gas by ultrasonic irradiations is more effective than removal by evacuation. The first mechanism mentioned above, i.e., direct gas detrapping from a $X_n(g)$ nucleus by ultrasound, would explain this greater efficiency. We have not yet obtained any evidence for the second mechanism of the destruction of X_n nuclei above, i.e., by mechanical disintegration. However, this possibility should still be kept in mind; it could be that irradiation of a liquid for much longer times than used here results in the mechanical destruction of nuclei.

In conventional sonochemical experiments, as have been carried out by us and many other groups, continuous ultrasound is applied for a relatively long time (generally several minutes) and the integral yield is then determined by chemical analysis. This yield does not give any information about the ability of a liquid to cavitate as the irradiation times applied are very much longer than the time required for the inception of full cavitation. Similarly, in cavitation threshold measurements in which a chemical effect, luminescence, or scattering is measured as a function of intensity or pulse length,^{9,10} one is dealing with the stationary situation attained after a certain time of cavitation buildup. The pulse train experiments reported here tackle a new aspect of the inception of cavitation: its buildup before the stationary state is reached.

Ultrasound is used in the form of short-pulse trains in various medical applications. It has previously been shown that such pulses can also initiate chemical reactions under in vitro conditions in solutions which are saturated by a gas such as air or argon.^{11,12} There is a lot of debate about the possibility of cavitation in biological tissue.¹³ The present results add a new aspect to this discussion: the cavitation ability is decreased when a liquid is not fully saturated by a gas.

The improvement of the cavitation behaviour of the luminol solution upon aging as shown in Figure 1 is most puzzling. The effect is not due to the aging of water as the same effect was observed when the solution was prepared using aged water. One must suspect that the improved ability of the solution to cavitate is connected to the dissolution of the solid compounds, i.e., luminol and sodium hydroxide. These compounds possibly introduce solid dust particles into the solution which can develop into cavitation

(5) Crum, L. A. *Appl. Sci. Res.* **1982**, *38*, 101.

(6) Gutiérrez, M.; Henglein, A. *J. Phys. Chem.* **1990**, *94*, 3625.

(7) Eller, A. I.; Flynn, H. G. *J. Acoust. Soc. Am.* **1965**, *38*, 493.

(8) Crum, L. A. *J. Acoust. Soc. Am.* **1980**, *68*, 203.

(9) Fowlkes, J. B.; Crum, L. A. *J. Acoust. Soc. Am.* **1988**, *83*, 2190.

(10) Atchley, A. A.; Frizzell, L. A.; Apfel, R. E.; Holland, C. K.; Mandanshetty, S.; Roy, R. A. *Ultrasonics* **1988**, *26*, 280.

(11) Carmichael, A. J.; Mossoba, M. M.; Riesz, P.; Christman, C. L. *IEEE Transactions* **1986**, *UFFC-33*, 148.

(12) Henglein, A.; Gutiérrez, M.; Ulrich, R. *Int. J. Radiat. Biol.* **1988**, *54*, 123.

(13) Williams, A. R. *Ultrasound: Biological Effects and Potential Hazards*; Academic Press: New York, 1983; p 148.

nuclei $X_n(g)$ with aging. The aging process could consist of the formation of agglomerations of dust particles, a single dust particle possibly not having a crevice to stabilize a gas pocket. The experiments of Figure 1 show once more that the inception of cavitation by ultrasound is decisively determined by the pre-

treatment of the solution.

Acknowledgment. We thank Dr. J. Lilie and Dr. E. Janata for technical advice. This work was supported by Deutsche Forschungsgemeinschaft und Fonds der Chemischen Industrie.

Negative Ion Photoelectron Spectroscopy of HCF^- , $HCCl^-$, HCB^- , and HCI^- : Photoelectron Angular Distributions and Neutral Triplet Excitation Energies

Mary K. Gilles, Kent M. Ervin,[†] Joe Ho, and W. C. Lineberger*

Joint Institute for Laboratory Astrophysics, University of Colorado and National Institute of Standards and Technology, and Department of Chemistry and Biochemistry, University of Colorado, Boulder, Colorado 80309-0440 (Received: August 2, 1991)

Photoelectron spectra and angular distributions are reported for the $H CX(^1A') + e^- \leftarrow H CX(\tilde{X}^2A'')$ and $H CX(^3A'') + e^- \leftarrow H CX(\tilde{X}^2A'')$ transitions of the halocarbenes ($X = F, Cl, Br, \text{ and } I$). Taking photoelectron spectra at parallel and perpendicular laser polarizations with respect to the direction of the photoelectron detection allows us to distinguish the triplet transition from the overlapping singlet transition. Ab initio calculations used to simulate the Franck-Condon envelope for the triplet states combined with the experimental data predict that HCl has a triplet ground state. Best estimates for the triplet excitation energy based on these simulations are 14.9 ± 0.4 kcal/mol (HCF), 4.2 ± 2.5 kcal/mol ($HCCl$), 2.6 ± 2.2 kcal/mol (HCB), and -2 to -10 kcal/mol (HCI). Vibrational intervals of 850 ± 60 cm^{-1} ($HCCl$), 725 ± 70 cm^{-1} (HCB), and 637 ± 80 cm^{-1} (HCI) in the $H CX(^3A'') + e^- \leftarrow H CX(\tilde{X}^2A'')$ transitions are attributed to the C-X stretch of the neutral. Adiabatic electron affinities for the singlet states are found to be 0.542 ± 0.005 (HCF), 0.535 ± 0.005 (DCF), 1.210 ± 0.005 ($HCCl$), 1.454 ± 0.005 (HCB), and 1.680 ± 0.005 eV (HCI). The electron affinity of 3HCl is expected to lie between 1.25 and 1.59 eV. Asymmetry parameters are also reported for photoelectrons from F^- , Br^- , and I^- ($h\nu = 351.1$ nm).

I. Introduction

Carbenes have intrigued chemists for a number of decades, with their fascinating chemistry,¹⁻³ two low-lying electronic states, and their challenge to ab initio theory. Interesting problems include the determination of carbene geometries, ground-state multiplicities, and the energy difference between the low-lying $^1A'$ and $^3A''$ states. The chemistry is quite different for these two states. For example, singlet methylene undergoes stereospecific cis addition to olefins while triplet-state methylene undergoes nonstereospecific addition to olefins. In the early studies of carbene chemistry the degree of stereospecificity in reactions with olefins was used to infer the ground spin state of the carbene.^{2,4-6} Later these types of reactions were used to determine that HCF ,⁷ $HCCl$,⁸ and HCB ⁹ possessed $^1A'$ ground states.

The halocarbenes ($H CX$) have been the subject of many ab initio calculations, both on the \tilde{X}^1A' state geometries for HCF ,¹⁰⁻¹⁸ $HCCl$,¹⁴⁻¹⁷ and HCB ¹⁴⁻¹⁶ and their \tilde{a}^3A'' state geometries.¹⁰⁻¹⁵ Computations by Bauschlicher et al.¹⁴ including configuration interaction obtained geometries and vibrational frequencies for the ground-state singlet and low-lying triplet spin states of HCF , $HCCl$, and HCB . Scuseria et al.¹⁶ determined molecular geometries and frequencies for the lowest singlet and triplet states of HCF , $HCCl$, and HCB using triple- ζ plus double polarization basis sets. Geometries, frequencies and force fields for the \tilde{X}^1A' and the \tilde{a}^3A'' states of HCF were computed by Weis et al.¹⁰ using highly correlated electron wave functions. Tomonari et al.¹¹ obtained geometries, frequencies, and force fields for the \tilde{X}^1A' and the \tilde{a}^3A'' neutral states of HCF and for the \tilde{X}^2A'' state of HCF^- . Predictions for the HCF triplet excitation energy have varied from 0 to 26.7 kcal/mol.^{10-15,19-25} Recent calculations by Weis et al.¹⁰ and Shin et al.²⁵ predict the energy difference between the lowest singlet and triplet states to be 13.9 and 14.5 kcal/mol,

respectively. Additional computations on $HCCl$ ^{14-16,23,24,26} and HCB ^{14,16} predict that the triplet excitation energy decreases in

- (1) Gaspar, P. P.; Hammond, G. S. In *Carbene Chemistry*; Kirmse, W., Ed.; Academic: New York, 1964; Chapter 12.
- (2) Gaspar, P. P.; Hammond, G. S. In *Carbenes*; Moss, P. A., Jones, Jr. M., Eds.; Wiley-Interscience: New York, 1975; Chapter 6.
- (3) Gilchrist, T. L.; Rees, C. W. *Carbenes, Nitrenes, and Arynes*; Appleton-Century-Crofts: New York, 1969; Chapter 6.
- (4) Skell, P. S.; Klebe, J. J. *Am. Chem. Soc.* **1960**, *82*, 247.
- (5) Skell, P. S.; Woodworth, R. C. *J. Am. Chem. Soc.* **1956**, *78*, 4496.
- (6) Skell, P. S.; Woodworth, R. C. *J. Am. Chem. Soc.* **1956**, *78*, 6427.
- (7) Woodworth, R. C.; Skell, P. S. *J. Am. Chem. Soc.* **1959**, *81*, 3381.
- (8) Closs, G. L. In *Topics in Stereochemistry*; Eliel, E. L., Allinger, N. L., Eds.; Wiley: New York, 1968; p 193.
- (9) Tang, Y.; Rowland, F. S. *J. Am. Chem. Soc.* **1967**, *89*, 6420.
- (10) Hine, J. *Divalent Carbon*; Ronald Press: New York, 1964; p 75.
- (11) Closs, G. L.; Coyle, J. J. *J. Am. Chem. Soc.* **1965**, *87*, 4270.
- (12) Weis, B.; Rosmus, P.; Yamashita, K.; Morokuma, K. *J. Chem. Phys.* **1990**, *92*, 6635.
- (13) Tomonari, M.; Almlöf, J.; Taylor, P., private communication.
- (14) Baird, N. C.; Taylor, K. F. *J. Am. Chem. Soc.* **1978**, *100*, 1333.
- (15) Staemmler, V. *Theor. Chim. Acta* **1974**, *35*, 309.
- (16) Bauschlicher, Jr., C. W.; Schaefer III, H. F.; Bagus, P. S. *J. Am. Chem. Soc.* **1977**, *99*, 7106.
- (17) Hoffmann, R.; Zeiss, G. D.; Van Dine, G. W. *J. Am. Chem. Soc.* **1968**, *90*, 1485.
- (18) Scuseria, G. E.; Durán, M.; MacLagan, R. G. A. R.; Schaefer III, H. F. *J. Am. Chem. Soc.* **1986**, *108*, 3248.
- (19) Mueller, P. H.; Rondan, N. G.; Houk, K. N.; Harrison, J. F.; Hooper, D.; Willen, B. H.; Liebman, J. F. *J. Am. Chem. Soc.* **1981**, *103*, 5049.
- (20) Carter, E. A.; Goddard III, W. A. *J. Chem. Phys.* **1988**, *88*, 1752.
- (21) Goldfield, D.; Simons, J. *J. Phys. Chem.* **1981**, *85*, 659.
- (22) Luke, B. T.; Pople, J. A.; Krogh-Jespersen, M.-B.; Apeloig, Y.; Karnie, M.; Chandrasekhar, J.; Schleyer, P. v. R. *J. Am. Chem. Soc.* **1986**, *108*, 270.
- (23) Dixon, D. A. *J. Phys. Chem.* **1986**, *90*, 54.
- (24) Harrison, J. F. *J. Am. Chem. Soc.* **1971**, *93*, 4112.
- (25) Carter, E. A.; Goddard III, W. A. *J. Phys. Chem.* **1987**, *91*, 4651.
- (26) Carter, E. A.; Goddard III, W. A. *J. Phys. Chem.* **1986**, *90*, 998.
- (27) Shin, S. K.; Goddard III, W. A.; Beauchamp, J. L. *J. Chem. Phys.* **1990**, *93*, 4986.

* To whom correspondence should be addressed.

[†] Present address: Department of Chemistry, University of Nevada, Reno, NV 89557-0020.